COMPUTER METHODS AND PROGRAMS IN BIOMEDICINE 104 (2011) 418–425

journal homepage: www.intl.elsevierhealth.com/journals/cmpb

A contextual based double watermarking of PET images by patient ID and ECG signal

Mohammad-Saleh Nambakhsh[a], Alireza Ahmadian[b,*], Habib Zaidi[c]

[a] Department of Biomedical Engineering, The University of Western Ontario, and Imaging Research Laboratories, Robarts Research Institute, London, Ontario, Canada
[b] Department of Biomedical Systems & Medical Physics, Tehran University of Medical Sciences and Research Center for Science and Technology in Medicine, Tehran, Iran
[c] Geneva University Hospital, Division of Nuclear Medicine, CH-1211 Geneva, Switzerland

ARTICLE INFO

Article history:
Received 17 December 2008
Received in revised form
25 August 2010
Accepted 25 August 2010

Keywords:
Watermarking
Medical images
ECG
Patient demographic text
Wavelet transform

ABSTRACT

This paper presents a novel digital watermarking framework using electrocardiograph (ECG) and demographic text data as double watermarks. It protects patient medical information and prevents mismatching diagnostic information. The watermarks are embedded in selected texture regions of a PET image using multi-resolution wavelet decomposition. Experimental results show that modifications in these locations are visually imperceptible. The robustness of the watermarks is verified through measurement of peak signal to noise ratio (PSNR), cross-correlation (CC%), structural similarity measure (SSIM) and universal image quality index (UIQI). Their robustness is also computed using pixel-based metrics and human visual system metrics. Additionally, beta factor (β) as an edge preservation measure is used for degradation evaluation of the image boundaries throughout the watermarked PET image. Assessment of the extracted watermarks shows watermarking robustness to common attacks such as embedded zero-tree wavelet (EZW) compression and median filtering.

1. Introduction

The huge amounts of acquired digital medical images in hospitals are usually stored in a database along with the demographic text data and the bio-signals of patients. Unauthorized tampering, mismatching and mishandling of information are problems with such data in large databases. Additionally, exchange of bio-signals, demographic texts and medical images between hospitals needs efficient and reliable transmission and storage techniques. Moreover, storing different information of a patient in separate files increases the risk of mismatching and diagnostic mistakes. Unauthorized viewing of patients' healthcare information is one of the main concerns in hospital information systems.

Recently, watermarking has been an active area of research for strengthening healthcare information security. Generally, watermarking algorithms have been aimed to protect digital images by hiding information into them. The main advantage of watermarking is information invisibility and anonymity. Authentication is considered a genuine application for them. A large number of watermarking techniques for medical images are available in literature which almost most of them focus on two areas, namely, tamper detection and authentication, and electronic patient record (EPR) embedding in medical images. Significantly, embedding of EPR or metadata

* *Corresponding author*. Tel.: +98 9123197825/98 21 66466383; fax: +98 21 66466383.
E-mail addresses: mnambak@uwo.ca (M.-S. Nambakhsh), ahmadian@sina.tums.ac.ir (A. Ahmadian), habib.zaidi@hcuge.ch (H. Zaidi).
0169-2607/$ – see front matter
doi:10.1016/j.cmpb.2010.08.016

in medical images saves memory of the hospital information system (HIS), enhances confidentiality of the patient data, avoid detachment of the EPR data from the image and saves bandwidth for transmission [1–3,12]. An extensive literature review in [12] shows multiple watermarking of medical images aims to provide a unified approach to different healthcare applications and is quite a creative concept.

The watermarking methods can be distinctly classified as transform domain techniques [4–6], spatial domain [7,8], selectable domain techniques [9], and combinational domain techniques [10]. One special approach is inserting an encrypted electronic patient record in the LSB of pixels' gray level [11]. The advantage and disadvantage of the approach are least visual modification of medical images, and the fact that LSB-embedding is known as a fragile method, respectively. To increase robustness of spatial domain techniques, wavelet-based watermarking methods exploit the frequency and spatial information of the transformed data in multiple resolutions. Currently applied wavelet-based digital watermarks are found in [4–6,12–15]. The advantages of the wavelet transform compared to the discrete cosine transform (DCT) and the discrete Fourier transform (DFT) are discussed in details elsewhere [15]. We recently exploited the embedded zero-tree wavelet (EZW) algorithm for a blind watermarking of bio-signals into medical images [13]. Meanwhile, perceptual models, the human visual system (HVS), texture properties or reference register (RR) [16] can be exploited to enhance watermark-embedding methods.

Texture as a function of spatial variation in pixel intensities is a significant feature commonly used for detection of embedding sites [17]. Wavelet analysis is particularly useful for texture perception. It may provide scale-dependent texture properties of the image to be targeted for any further processing [18]. To preserve medical images, invertible watermarking allows the recovery of the original image without any loss of information [19]. Another alternative is the selection of regions of interest (ROIs) which contains diagnostic significance to be left intact during watermarking procedure [19].

In this paper, we propose a contextual double digital watermarking technique using ECG signal and patient ID as watermarks to be inserted into PET images. The insertion locations are selected using a texture feature extraction algorithm to provide acceptable imperceptibility of the watermarked image. Combination of texture algorithm with the wavelet transform makes the method more effective for medical watermarking applications. The following sections describe the process of embedding ECG signal and patient ID image into selected texture regions of the clinical PET images.

2. Proposed watermarking algorithm

In this paper, the ECG signal and the text image (patients ID) are used as double contextual watermarks. They are embedded into the PET image. The PET modality is used particularly because of its availability, but any other kind of medical image can be used. The grayscale PET image is decomposed to seven sub-bands using a two-level dyadic wavelet decomposition as shown in Fig. 1. The wavelet coefficients of both the ID text image and the ECG signal are embedded into these two-dimensional wavelet sub-bands.

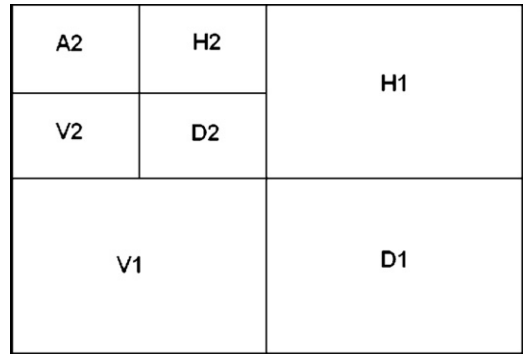

Fig. 1 – Schematic representation of the two-level wavelet decomposition technique.

Although considering an ROI in a significant part of PET image may enrich work to avoid degradation of diagnostically important section of the image, we did not take it into account and left it for future studies. Usually, ROIs are defined when a significant region of the image must be untouched and archived for further diagnosis. Otherwise an extended region of the image can be exploited for watermarking [19]. While considering ROIs more caution must be taken in order to not distort clinically meaningful parts of the selected region of the image.

2.1. *Texture extraction of PET image*

Let M be an $N \times N$ input grayscale image in the spatial domain. M is transformed to the wavelet domain using the Haar mother wavelet. The Haar wavelet is very simple, fast and invertible wavelet transform. The Haar coefficients are dyadic rational numbers with denominators of power of 2 so that LSB watermarking of decomposed image coefficients guarantees lossless reversibility of watermark coefficients. In other words, the ECG signal and ID watermarks are preserved in the process of Haar wavelet reconstruction and decomposition of PET image. Nonetheless, any other lossless wavelet can be used for this study, but it might impact on the precision of the ECG signal and the ID.

The decomposed image consists of three sub-bands (V, H and D) from which the texture information of image M at different scales and resolutions can be obtained. The resulting texture feature matrix is of dimension $N/(2^r) \times N/(2^r)$, which is the same as the corresponding sub-band matrixes, where r is the level of decomposition. The texture map (tw_r), is a matrix which shows texture areas superimposed on a background (non-texture pixels), which is computed for each input sub-band (w_r). The texture of each wavelet coefficient is calculated from a combination of its energy with the variance of the corresponding coefficients in the lowest wavelet approximation matrix (A). The process of obtaining texture features from an image was adopted from [20]. For two-levels decomposition, tw_r is obtained by

$$tw_r(i,j)=[w_r(i,j)]^2+\sigma^2[A_2([i/2]+1, \ [j/2]+1), \ A_2([i/2]+2, \ [j/2]+2)] \quad (1)$$

where σ^2 is the variance of the two-coefficient block and $w_r \in \{D_2, H_2, V_2, D_1, H_1, V_1\}$, A_2 is the approximation sub-band in the last scale, i and j are coordinates of pixels in each sub-band and [] the real part of a complex number. The i,j are in the span $1 \leq i, j \leq N/(2^r)$ to cover all image pixels.

The background pixels (pixels are not selected as texture) in the texture map have a lower magnitude compared to pixels representing the edge areas of the PET image. The locations in the texture map whose magnitude are higher than a predefined threshold, T_w, are selected for the watermarking process. Modification of these coefficients is imperceptible since the most significant coefficients act as a visual mask. The selected texture regions of D_1, V_1 and H_1 sub-bands are denoted by SEL_{D_1}, SEL_{V_1},and SEL_{H_1}:

$$\begin{aligned} &\mathrm{SEL}_{H_1} = \max[tw_{H_1}(i,j), tw_{H_1}(i,j+1)] \\ &\text{if } |tw_{H_1}(i,j) - tw_{H_1}(i,j+1 > T_{H_1} \\ &\mathrm{SEL}_{V_1} = \max[tw_{V_1}(i,j), tw_{V_1}(i+1,j)] \\ &\text{if} |tw_{V_1}(i,j) - tw_{V_1}(i+1,j)| > T_{V_1} \\ &\mathrm{SEL}_{D_1} = \max[tw_{D_1}(i,j), tw_{D_1}(i+1,j+1)] \\ &\text{if } |tw_{D_1}(i,j) - tw_{D_1}(i+1,j+1)| > T_{D_1} \end{aligned} \tag{2}$$

where the threshold in each sub-band is achieved by the equations given below:

$$\begin{aligned} T_{H_1} &= \max(tw_{H_1}) - \mathrm{avg}(tw_{H_1}) \\ T_{V_1} &= \max(tw_{V_1}) - \mathrm{avg}(tw_{V_1}) \\ T_{D_1} &= \max(tw_{D_1}) - \mathrm{avg}(tw_{D_1}) \end{aligned} \tag{3}$$

where T is interpreted as the deviation of the maximum coefficient from the mean of each sub-band. The average of each sub-band is the global information of the each sub-band and the maximum coefficient is a visual estimation of the sub-band's tolerance of degradation.

2.2. *Sub-band selection*

The sub-band selection for watermarking is trivial. Manipulation of the low frequency sub-band A_2 will impose severe degradations on the reconstructed image as most of the energy is concentrated in this sub-band.

Generally, high frequency sub-bands are responsible for image sharpness and watermark transparency, less watermark robustness, but they are larger in size so they provide more locations for watermark embedding. On the other hand, mid-frequency sub-bands provide more suitable places for watermarking while having less capacity and less transparency. In the meantime, they increase the risk of noticeable differences in the watermarked image. Therefore, a sort of trade-off should be considered for the embedding process to reach an imperceptible and robust watermarked image. The three mid-frequency sub-bands (H_2, V_2 and D_2) were found to be empirically good choices for the ECG. Unlike the ECG signal, the significant coefficients of the ID image are embedded into the high frequency sub-bands.

2.3. *Embedding the ECG signal*

The wavelet coefficients of ECG signal are embedded into the selected texture regions of the V_2, H_2 and D_2, respectively. The size of the ECG is adjusted to be one third of the total number of available embedding locations. The scanning of the candidate location during embedding process is a well-known predetermined scanning methods which is called Morton scan [13,21]. The ECG coefficients are chosen by the Morton or Raster scan method as well [13]. The embedding stopping point is the time by which most significant ECG's wavelet coefficients are running out.

Let the ECG signal be of size $1 \times P$, where P is number of ECG bytes in time domain. The wavelet coefficients of the ECG, W_f, are divided into three bit-streams, L, I, and M, representing the least-significant, the intermediate, and the most significant decimal values, respectively, as shown in Eq. (4):

$$W_f(i,j) = 100 \times M(i,j) + 10 \times I(i,j) + L(i,j) \tag{4}$$

where $0 \leq (L, I) \leq 9$ and $0 \leq M \leq \max(W_f)/100$. The bit-streams L, I and M are inserted into the lowest order bits of SEL_{V_2}, SEL_{H_2} and SEL_{D_2} according to an order that is selected by secret key.

The secret key includes the seeds of pseudorandom number generator (3 bytes), type of mother wavelet (2 bytes), number of ECG bytes (2 bytes), size of original ID image (2 bytes), T in Eq. (3) (3 bytes), seeds for random specifying of sub-bands' order (1 byte) in the embedding process. Regardless of PET image size the secret key is normally greater or equal than 13 bytes. They are arranged in a predefined order as a sequence of bits. It is also possible to encrypt the secret key for more security.

2.4. *Embedding the text image*

The patient ID image's wavelet coefficients (IDW) are embedded into the wavelet coefficients V_1, H_1 and D_1. Using a threshold (T), the binary matrix (BM) of each sub-band is made by assigning 0 to all coefficients bigger than T and 1 otherwise. The value of T is empirically set to one third of the maximum coefficient. Then, the BM is used to find candidates for watermarking from the IDW. The coefficients are scanned by Raster scan. Using this predetermined scan, only locations where their corresponding location in the BM is filled with 0 are chosen out for watermarking. Thus, from knowing the size of the ID, the Raster scan, and T in the extraction process the algorithm is able to place back every single extracted coefficient into its original location in the IDW and reconstruct the ID.

The text ID is converted to an image, because embedding characters in the wavelet domain is not plausible. Although there are some approaches to embed text characters in the form of binary into the wavelet coefficients of the PET image, it is much more robust to embed them into similar coefficients of the same trait and domain. Moreover, the largest concern is that a slight change in the binary sequence of a character can turn it entirely into another character. Therefore working with characters in the wavelet domain can diminish robustness of the watermark drastically. In the meantime, transforming the ID to an image and to the wavelet domain makes coefficients of the same characteristics as the transformed PET

Table 1 – Assessment of watermarks quality.

Watermarks	PSNR	Cross-correlation (%)	SSIM	UIQI
ECG	70.12 ± 0.12	93.36 ± 0.09	0.901 ± 0.07	0.910 ± 0.13
ID image	61.34 ± 0.16	91.05 ± 0.1	0.935 ± 0.13	0.913 ± 0.19

image (real numbers in almost the same range). Although this has the effect of raising the payload of watermarking, it also strengthens the ID watermark.

In the proposed method, the lowest order bits of SEL_{V_1}, SEL_{H_1} and SEL_{D_1} are replaced by the IDW bits of *L*, *I* and *M* according to the order that is selected by the secret key. It should be noted that the white background of the ID image is a worthless part of it, so the wavelet coefficients of this area are not embedded into the PET image.

2.5. *Watermarking of PET images*

The final watermarked PET image is obtained when the embedded sub-bands are reconstructed using a two-level inverse discrete wavelet transform (IDWT). After extracting texture map matrixes, using the Raster scan (Fig. 2a) all the extracted locations are numbered from 1 to *n* orderly in each individual sub-band, where *n* is the number of candidates for watermarking in each corresponding sub-band (Fig. 2b). Now a pseudorandom number generator given a seed generates a sequence of numbers between 1 and *n* for each sub-band. Seeds are the parameters being stored in the secret key of the watermarking algorithm. Also, the secret key is used to select the corresponding embedding sub-bands (*V*, *H* and *D*) for *L*, *I* and *M* of the ID image and the ECG signal in their mentioned scale randomly. Therefore, the secret key secures the embedded ECG and ID watermarks from disclosure. Fig. 3 shows the proposed watermarking algorithm used for embedding the ECG and the text images in the PET image.

The proposed algorithm was applied on 25 PET images (256 × 256). A typical image plane is shown in Fig. 4a. The original ECG signal and the ID image (32 × 32) used as contextual watermarks are shown in Fig. 4b and c, respectively. The resulting watermarked image is shown in Fig. 4d.

The experimental results presented are obtained using a set of cardiac images using [^{18}F]-fluorodeoxyglucose (FDG) PET images acquired at Geneva University Hospital on a dedicated clinical PET/CT scanner, namely the Biograph TruePoint 64 (Siemens Medical Solutions, Erlangen, Germany). The physical performance of this scanner and its application in a clinical setting is reported elsewhere [22] whereas the ID images and ECG signals are taken from the Massachusetts Institute of Technology database (MIT-DB) [23]. An experienced physician evaluated the perceptual quality of the watermarked and original images and did not report any remarkable visual difference.

3. Verifying the integrity of the watermarks

The extraction procedure is the reverse of the embedding process shown in Fig. 3. The same secret key that was used during embedding is now used to determine the order of extracting the coefficients. The watermark retrieving procedure needs to be aware of the location of embedded coefficients, IDW, in their original context (ECG, ID). Thus, the embedding clues are stored in the secret key to be used in the extraction or the retrieving procedure.

As explained in Eq. (3), watermark coefficients spilt up to *M*, *I*, *L* which are separately embedded in different sub-bands. This method guarantees reconstruction of a fairly equal coefficient compressed to the original one if even only *M* or *M* and *I* be able to be reconstructed. Therefore, this guarantees reliable extraction. The proposed watermarking is blind because neither the original PET image nor the original watermarks is required for extraction. The extracted ID and ECG are of good quality and closely resemble the original contents shown in Fig. 4b and c. The extracted patient's ECG is shown in Fig. 5, and the extracted ID image is shown in Fig. 4d.

The average cross-correlation between the extracted signal and the embedded one from all 25 watermarked PET images is 93.36%. This value is 91.05% for the ID image. These results show that acceptable extracted results with low error can be achieved using the proposed algorithm. In the reconstructed ID image, some characters are not completely extracted but are visually recognizable.

We quantitatively determined the degree of similarity between the original watermarks and the extracted watermarks using two different types of metrics. The peak signal to noise ratio (PSNR) and correlation between the original and the modified image give the pixel-based similarity between the images [24]. The structural similarity measure (SSIM) and universal image quality index (UIQI) [25,26] compare the images based on the human visual system (HVS). The cross-correlation (CC) [24] between the embedded ECG and the extracted one was used for similarity assessment. Table 1 summarizes the average degree of similarity between the five original ECG signals and the ID images and their corresponding extracted ones.

The similarity results using both the pixel-based approach and the human visual system approach show a high level of correlation between the images. Watermarks were shown to be robust and resilient when subjected to various attacks. We analyzed the effect of these attacks on the extracted ECG and the ID image for diagnostic purposes. The visual quality of the text and the ECG are used by the human visual metrics for

Table 2 – Human visual metrics of the extracted marks.

Attacks	ECG		ID Image	
	SSIM	UIQI	SSIM	UIQI
Median filter	0.76	0.89	0.94	0.96
EZW compression	0.80	0.87	0.93	0.94
Rotating	0.33	0.36	0.39	0.40

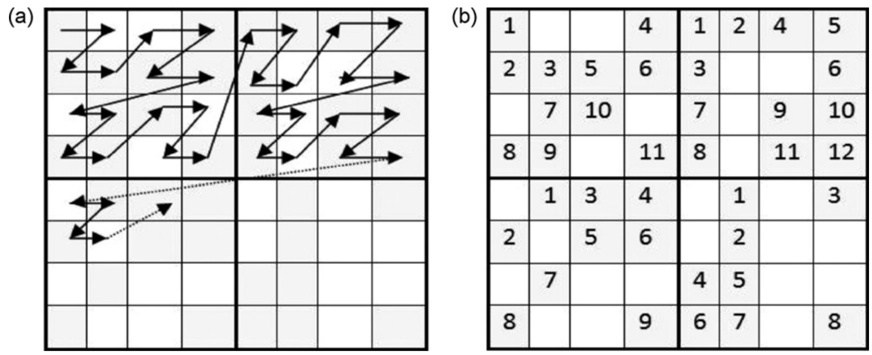

Fig. 2 – (a) Raster scan of wavelet matrix of an image, (b) numbering of gray locations (texture maps) in each sub-band separately.

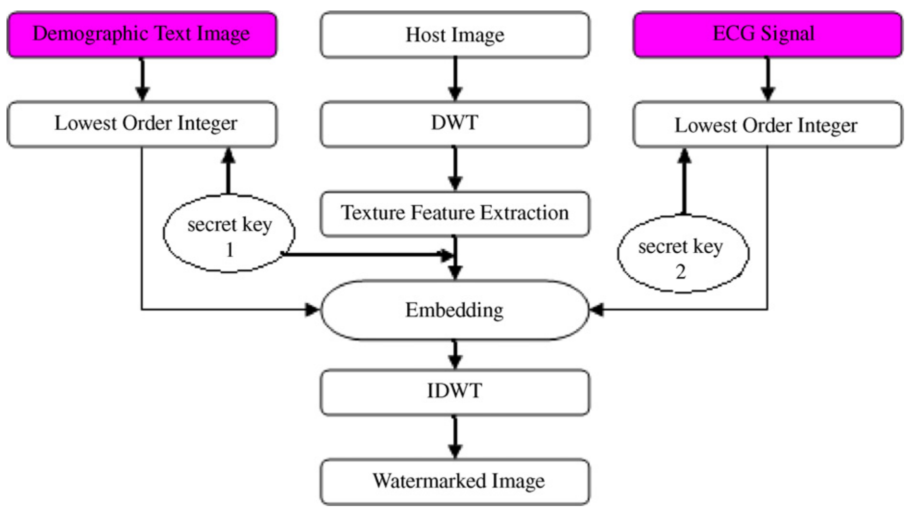

Fig. 3 – Proposed ECG and ID image watermarks embedding algorithm.

comparison purposes. Table 2 summarizes the human visual metrics of the extracted marks when the watermarked image is subjected to various attacks. Numerical results show that the image quality is high for all attacks except rotation which originates from the lack of synchronization in the process of embedding.

Hence, the watermarked PET image is compact and takes up less memory space compared to the memory that is occupied by the individual image and accompanying data separately. It should be noticed that changing the modality of medical image does not change any part of the algorithm but it might affect the evaluation results

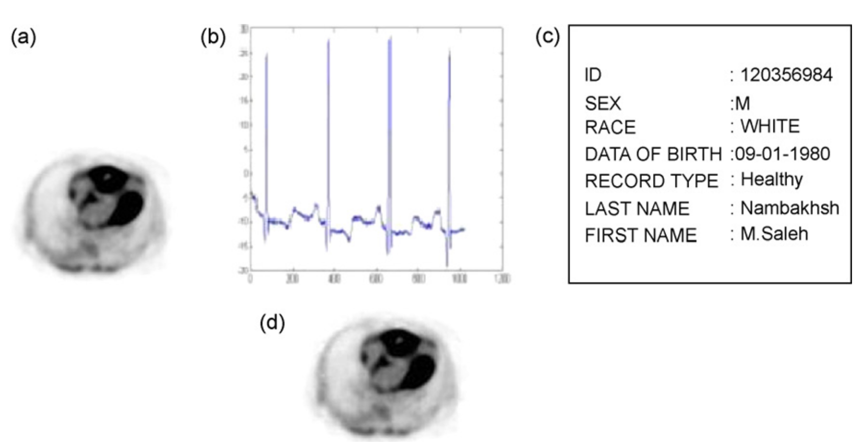

Fig. 4 – (a) Original PET image, (b) original ECG signal, (c) original ID image, and (d) watermarked PET image.

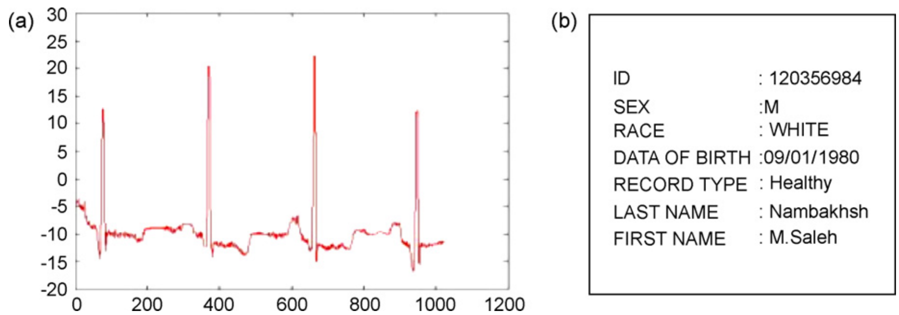

Fig. 5 – Result of the extracted (a) ECG signal and (b) the ID image.

Table 3 – Maximum capacity of each sub-band of a PET image for watermarks according to texture algorithm.

Sub-bands	Capacity (number of embeddable bits)	Watermarks
V_1	24,543	ID image
H_1	23,401	ID image
D_1	20,129	ID image
V_2	8993	ECG signal
H_2	9800	ECG signal
D_2	6520	ECG signal

because different modalities have different texture content.

4. Performance of the watermarking algorithm

The developed algorithm was applied on 25 different PET images (256 × 256). Table 3 shows the sub-bands used for each watermark and its corresponding capacity of modulation. For quality assessment of the watermarked PET, the average PSNR between the original image and the watermarked image was calculated. This value was found to be more than 47.43 dB with a standard deviation of 0.22 dB for embedding an ECG 1 kbyte in size, as shown in Fig. 6 (5 samples are illustrated for better presentation). The PSNR provides an overall efficient numerical measure of image distortion which imparts important information in medical applications. To measure the visual degradation of the watermarked PET image, SSIM and UIQI parameters were calculated which were 0.93 and 0.96, respectively.

From a clinical point of view, it is a routine procedure to record 1–4 min of ECG with 360 samples per second. This makes the storage size in the range of 21.6–86.4 kbytes. However, the ECG signal has a great amount of redundant data as some of its main features such as the QRS complex are used for many diagnoses procedures. There are many algorithms that compress ECG signal in the range of 20:1 ratio [27,28]. Hence, with the proposed algorithm, it is possible to embed real ECG signal records of a patient (1–4 min) in his/her medical images.

As it is shown in Fig. 6, the PSNR graph has a steep descent versus the ECG signals larger than 1024. It stems from the small size of the subject PET images (256 × 256). The algorithm achieves good results for up to 1024 ECG bytes. Thus, for the PET images of 256 × 256 size, the proposed algorithm embeds the ECG signals smaller than 1024 bytes perfectly. The proposed method is compared with the method described in [12] which watermarks PET images with size 512 × 512 using four different watermarks. Both studies are based on Haar wavelet, for multiple watermarking. Despite the watermarks difference, the two images are considered roughly comparable in terms of capacity of watermarks and their impact on the host image. In [12], the watermarks are inserted in different decomposition scales and sub-bands, in locations specified by a random key, depending on their type. In this study, two more medical applicable watermarks are inserted into sub-bands of the first two scales. The insertion was based on invisibility of the watermarks after watermarking. The average PSNR reported in [12] was 46.66 ± 0.2 for nearly 668 bytes (5348 bits) of watermarks. While, the proposed algorithm achieved PSNR equal to 48.15 ± 0.22 for 2 kbytes of watermarks (ECG and ID). Moreover, the host PET image used in [12] is of size 512 × 512 while in this study it is 256 × 256.

A comparison between the distortions induced by applying watermarks and by image compression is a sound indicative of the amount of distortion PET image was undergone by the proposed watermarking method. Table 4 presents comparative evaluations of the distortions in terms of PSNR induced

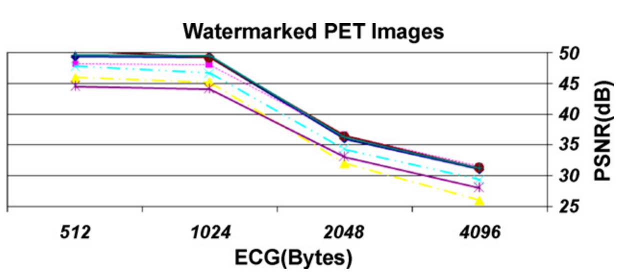

Fig. 6 – Plot of PSNR (peak signal to noise ratio) vs. ECG size for five images having different textures and content.

Table 4 – Performance of watermarked and JPEG images in terms of PSNR.

Image processing type	QF	PSNR (dB)
Watermarked image	–	48.33
JPEG compressed image	90	51.65
	85	48.30
	70	46.12
	65	40.32

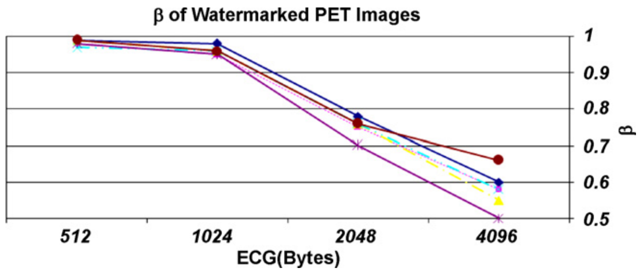

Fig. 7 – Plots of β factor (edge preservation measure) vs. ECG size for five images having different textures and content.

by applying the embedding scheme and JPEG compression as an indicative attack with different quality factors (QFs) applied to the whole image. As illustrated in Table 4, the watermarking method introduces less distortion than the JPEG compression with quality factors up to 85. The adequate perceptual quality of the watermarked images, combined with the high PSNR obtained, demonstrates the transparency of the proposed scheme.

Moreover, the beta factor (β) is an edge preservation measure used for evaluation of the boundary degradation throughout the image. Normally, a β close to 1 is interpreted as low degradation. The β factor of the watermarked PET image is calculated using Eq. (5) and shown in Fig. 7.

$$\beta = \frac{\sum\sum[(\Gamma I - \bar{\Gamma} I)(\Gamma wI - \Gamma \bar{w}I)]}{\sqrt{\sum\sum(\Gamma I - \bar{\Gamma} I)^2(\Gamma wI - \Gamma \bar{w}I)^2}} \quad (5)$$

where ΓI is the high passed Laplacian filter of the original image, $\bar{\Gamma} I$ is its mean value and wI, $\bar{w}I$ is the watermarked and mean value of the watermarked image.

The achieved β for all experiments and ECG sizes less than 1024 bytes proves that we observe normal changes in the edge areas up to the above-mentioned size. As discussed earlier, because of the small size of PET images (256 × 256) and accordingly small area of significant coefficients or non-background, the algorithm is able to achieve good results for ECG sizes less than 1024. For higher ECG sizes, there is nearly a linear reduction in the β factor.

5. Conclusion

A contextual PET image watermarking algorithm was proposed. Two watermarks, an ECG signal and the corresponding demographic text data (ID) of a patient were embedded into selected texture regions of a host image in the wavelet domain. The watermarked PET image provides security of information. The robustness of the watermarks was not affected by common attacks like EZW compression and median filtering. Quantitative results show that the extracted ECG and ID image are of high quality. This is a result of utilizing texture areas of the host image which are the most significant areas of the medical image. Meanwhile, the use of these features should be done with caution owing to their possible diagnostic significance.

The combination of different information as proposed by the watermarking algorithm introduces easier data accessibility when practitioners need patient's healthcare history and other vital signs along with a medical image. The comparison of our method with a previously published wavelet-based method [12] shows reasonable improvement of the PSNR. The experimental results also prove that higher quality watermarked images can be achieved as compared to JPEG compressed images up to quality factor of 85%.

Acknowledgment

Thanks Brandon Miles for his helps. The authors would like to thank RCSTIM for supporting this project.

REFERENCES

[1] G. Coatrieux, C. Le Guillou, J. Cauvin, C. Roux, Reversible watermarking for knowledge digest embedding and reliability control in medical images, Trans. Info. Tech. Biomed. 13 (March (2)) (2009) 158–165.

[2] H. Munch, U. Englemann, A. Schroter, H.P. Meinzer, The integration of medical images with the patient record and their web based distribution, J. Acad. Radiol. 11 (2004) 661–668.

[3] G. Coatrieux, J. Montagner, H. Huang, C. Roux, Mixed reversible and RONI watermarking for medical image reliability protection, IEEE Int. Conf. Eng. Med. Biol. Soc. (EMBS) (2007) 5653–5656.

[4] A.A. Reddy, B.N. Chatterji, A new wavelet based logo-watermarking scheme, Pattern Recogn. Lett. 26 (2005) 1019–1027.

[5] T.J.S. Cho, S.W. Shin, W.H. Lee, J.W. Kim, J.U. Choi, Enhancement of robustness of image watermarks embedding into colored image, based on WT and DCT, in: Proceedings of International Conference on Information Technology: Coding and Computing, Las Vegas, USA, 2000, pp. 483–488.

[6] M.-S. Hsieh, D.-C. Tseng, Y.-H. Huang, Hiding digital watermarks using multiresolution wavelet transform, IEEE Trans. Ind. Electron. 48 (2001) 875–882.

[7] B. Gunsel, U. Uludag, A.M. Tekalp, Robust watermarking of fingerprint images, Pattern Recogn. 35 (2002) 2739–2747.

[8] D.P. Mukherjee, S. Maitra, S.T. Acton, Spatial domain digital watermarking of multimedia objects for buyer authentication, IEEE Trans. Multimedia 6 (2004) 1–15.

[9] Yi-Ta. Wu, F.Y. Shih, An adjusted-purpose digital watermarking technique, Pattern Recogn. 37 (2004) 2349–2359.

[10] F.Y. Shih, S.Y.T. Wu, Combinational image watermarking in the spatial and frequency domains, Pattern Recogn. 36 (2003) 969–975.

[11] D. Anand, U.C. Niranjan, Watermarking medical images with patient information, In Proceedings of the 20th Annual International Conference of the IEEE Engineering in Medicine and Biology Society, 2(1998), 703–706.

[12] A. Giakoumaki, S. Pavlopoulos, D. Koutsouris, Secure efficient health data management through multiple watermarking on medical images, Med. Biol. Eng. Comput. 44 (2006) 619–631.

[13] M.S. Nambakhsh, A. Ahmadian, M. Ghavami, R. Dilmaghani, A novel blind watermarking of ECG signals on medical

images using EZW algorithm, in: Proceeding of IEEE International Conference on Engineering in medicine and Biology Society, New York, 2006, pp. 3274–3277.

[14] E. Elbasi, A.M. Eskicioglu, A DWT-based robust semi-blind image watermarking algorithm using two bands, in: Proceedings of SPIE, 18th Annual Symposium on Electronic Imaging, Security, Steganography, and Watermarking of Multimedia Contents, San Jose, CA, 2006.

[15] S. Pereira, S. Voloshynovskiy, T. Pun, Optimized wavelet domain watermark embedding strategy using linear programming, in: Proceedings of SPIE on AeroSense, Orlando, Florida, USA, 2000, pp. 490–498.

[16] Yi-Ta. Wu, F.Y. Shih, Digital watermarking based on chaotic map and reference register, Pattern Recogn. 40 (2007) 3753–3763.

[17] R. Ni, Q. Ruan, H.D. cheng, Secure semi-blind watermarking based on iteration mapping and image features, Pattern Recogn. 38 (2005) 357–368.

[18] M. Kociolek, A. Materka, M. Strzelecki, P. Szczypinski, Discrete wavelet transform-derived features for digital image texture analysis, in: Proceedings of the International Conference on Signals and Electronic Systems, 2001, pp. 163–168.

[19] T.A. Giakoumaki, S. Pavlopoulos, D. Koutsouris, Multiple image watermarking applied to health information management, IEEE Trans. Inf. Technol. Biomed. 10 (2006) 722–732.

[20] A.S. Lewis, G. Knowles, Image compression using the 2D wavelet transform, IEEE Trans. Image Process. 1 (2) (1992) 244–250.

[21] E. Artyomov, Y. Rivenson, G. Levi, O. Yadid-Pecht, Morton, (Z) scan based real-time variable resolution CMOS image sensor, IEEE Trans. Circuits Syst. Video Technol. 15 (7) (2005) 947–952.

[22] H. Zaidi, F.O. Schoenahl, Ratib Geneva PET/CT facility: design considerations and performance characteristics of two commercial (Biograph 16/64) scanners, Eur. J. Nucl. Med. Mol. Imaging 34 (Suppl. 2) (2007) S166.

[23] Available from: http://www.physionet.org/physiobank/databaseTH (accessed March 2006).

[24] W.-H. Lin, S.-J. Horng, T.-W. Kao, P. Fan, C.-L. Lee, Y. Pan, An efficient watermarking method based on significant difference of wavelet coefficient quantization, IEEE Trans. Multimedia 10 (August (5)) (2008) 746–757.

[25] W. Zhou, A.C. Bovik, H.R. Sheikh, E.P. Simoncelli, Image quality assessment: from error visibility to structural similarity, Image Process., IEEE Trans. 13 (April (4)) (2004) 600–612.

[26] D. Drajic, N. Cvejic, Adaptive fusion of multimodal surveillance image sequences in visual sensor networks, IEEE Trans. Consum. Electr. 53 (November (4)) (2007).

[27] B.S. Kim, S.K. Yoo, M.H. Lee, Wavelet-based low-delay ECG compression algorithm for continuous ECG transmission, IEEE Trans. Inf. Technol. Biomed. 10 (2006) 77–83.

[28] H.-H. Chou, Y.-J. Chen, Y.-C. Shiau, T.-S. Kuo, An effective and efficient compression algorithm for ECG signals with irregular periods, IEEE Trans. Biomed. Eng. 53 (2006) 1198–1205.